Evaluation on thermal stability of embankments with different strikes in permafrost regions

Chou Ya-ling [a],*, Sheng Yu [b], Wei Zhen-ming [c]

[a] School of Civil Engineering, Lanzhou University of Technology, Lanzhou 730000, China
[b] State key Laboratory of Frozen Soil Engineering, Cold and Arid Regions Environmental and Engineering Research Institute, Chinese Academy of Sciences, Lanzhou 730000, China
[c] State Key Laboratory of Natural Gansu, Lanzhou Institute of Geology, Chinese Academy of Sciences, Lanzhou 730000, China

ARTICLE INFO

ABSTRACT

The former studies on embankment in permafrost regions indicate that the maximum thawed depth on the embankment central line is regarded as the evaluation criterion, through which the roadbed thermal stability is evaluated. In fact, thermal effect problems associated with slope orientations result in the maximum thawed depth position being deviated in the roadbed transverse direction rather than thawed on the embankment central line. So the thermal stability of the permafrost embankment will highly have been changed. In this paper, the thermal stability of permafrost embankment is modeled with the assumption that the air temperature will be warmed up by 0.022 °C/a when the running time is 20 a and 50 a, respectively. Different roadbed surfaces, different embankment heights and different roadbed strikes are all analyzed. Surface material includes gravelly and asphalt. Embankment height ranges from 0 m to 5.0 m with a step of 0.5 m. For the embankment strike, east to west (EW), southwest to northeast (SW–NE), south to north (SN) and symmetric route are taken into consideration. There are several significant findings summarized from the calculated results. Firstly, for the embankments with the shady–sunny slope that there are hardly linear relations between the changes of natural permafrost table and artificial permafrost table and the heights of embankment. Secondly, there are three results when the running time is 20 a: a) with the completely symmetric thermal boundary conditions and under both the gravelly and asphalt surfaces, there are almost linear relations between the changes of permafrost table and the embankment height; b) under the gravelly surface, for embankments with sunny–shady slopes, there is no linear relation between the changes of permafrost table and the embankment height; c) under the asphalt surface, for embankments with sunny–shady slopes, if the embankment is not high enough there is a linear relation between the changes of permafrost table and the embankment height, but the thermal stability cannot be reached. Thirdly, when the running time is 50 a, the thermal stability of all embankments cannot be reached other than the symmetric strike under the gravelly surface. Finally, when designing an embankment, besides considering the minimum embankment height and the maximum embankment height, the *Yin-Yang Slope* effect should be taken into account.

© 2009 Elsevier B.V. All rights reserved.

1. Introduction

In permafrost regions, the construction of embankments will change the thermophysical features of the natural ground surface and atmosphere, and influence the thermodynamic and dynamic stability of frozen soil layers. Establishing high roadbeds was considered as a conventional measure to protect the permafrost from thawing (Cheng et al., 2003). So, the critical height of the embankment in permafrost regions has been studied by many researchers. The critical height of the embankment is composed of the minimum critical embankment height and the maximum critical embankment height. According to

the field data of the years 1979 and 1980 along the Qinghai–Tibet highway under asphalt surface, QTH Research Group (1983) found that there were linear relationships between the changes of permafrost table and the embankment height. Through studying the critical height of the embankment for the highway in the permafrost regions of the Tibetan Plateau, Huang (1983) set up linear regression equations between the changes of permafrost table and the embankment height by statistical method. From the field data of several decades along the Qinghai–Tibet highway and Qinghai–Kangding highway, Wu et al. (1988, 1998) concluded that there were linear relationships between the changes of the permafrost table and the embankment height. Through numerical simulation on both low temperature and high temperature permafrost embankment of the Tibetan Plateau, Li et al. (1998, 2005) reached a conclusion that there were linear relationships between the changes of the permafrost table

---

* Corresponding author. Tel.: +86 931 4967297; fax: +86 931 4967271.
E-mail address: chouyaling@lzb.ac.cn (C. Ya-ling).

and the embankment height under all the gravelly, concrete and the asphalt surfaces, respectively. Zhang et al. (2005) presented the linear regression equations between the changes of the permafrost table and the embankment height by numerical calculation. The roadbed thermal stability in the permafrost regions points that the artificial permafrost table is not lower than the natural permafrost table. Based on this principle of the roadbed thermal stability, the method of the minimum critical embankment height can be gained through the linear regression equations between the changes of the permafrost table and the embankment height, now.

The abovementioned studies only consider the situation that the thermal boundary condition is completely symmetric, that is, the maximum thawed depth under the embankment center is regarded as the evaluation criterion of the roadbed thermal stability. In fact, there is no embankment with completely symmetric thermal boundary conditions, and the maximum thawed depth is not always located in the embankment centric line. Feng-huo-shan section of Qinghai–Tibet highway extends from North to South, there was obvious thermal difference between the east slope and the west slope. According to the field data of the years 1985 and 1986 in this section, the mean temperature of the east slope was 2.4 °C higher than that of the west slope(Wu et al., 1988). After roadbeds have been built in the permafrost regions, thermal effect problems associated with slope orientations must also be considered in the protection measures of roadbed engineering (Cheng, 2003). By far, many numerical computations on the embankment temperature field in the permafrost regions have failed to take into account of the road strike, even the temperature of the slopes is lower than that of the surface (Zhang et al., 2006; Liu and Lai, 2004), which are still considered as symmetric thermal boundary conditions (Liu and Tian, 2002; Wen et al., 2005; Zhang et al., 2005). With regard to the embankment with completely symmetric thermal boundary conditions, the maximum thawed depth position is situated on the centric line of the roadbed. But for the embankment with shady–sunny slopes, the asymmetric thermal boundary conditions of the slopes result in the maximum thawed depth position being deviated from the embankment central line. The higher is the roadbed, the greater is the transverse thermal difference. Apparently, it is unreasonable to analyze permafrost thermal stability just according to the symmetric boundary conditions. The Chinese National highway 214 whose strike is 246° and the surface is asphalt and concrete. Although it is a road re-built in 2002, from the field data obtained from the section K369+000 to K369+100 along the Chinese National highway 214, we find that the mean annual temperature of the sunny slope is 4.22 °C higher than that of the shady slope, and many longitudinal cracks on the south side of the roadbed had occurred by the end of 2005. It is the main cause that differential deformations and settlements are induced by the transverse thermal difference, and longitudinal cracks that occurred on that side resulting from thaw settlement in the south-faced side are much larger.

There are many factors that contribute to the embankment thawing features in the permafrost regions. Influencing factors such as solar radiation, side drainage, snow accumulation, vegetation cover, cloud, precipitation and wind, complicate the embankment temperature field in the permafrost region, but the solar radiation is the key factor (Hu et al., 2002). On the Qinghai–Tibet Plateau, the fact is that the high altitude, thin and dry air, a great transparency factor, long sunlight hours, little rain, a short distance travelled by solar radiation and a hardly weakened solar radiation have to be considered(Sun, 2005). Field data (Chou et al., 2007)and associated documents (Sun et al., 2004) indicated that the temperature difference on slopes resulted principally from the difference in the amount of solar radiation on the slopes. So, when roadbeds are built in the permafrost regions, there will be different thermal regimes on the slopes because of different roadbed strikes. Some researchers have already paid attention to various thawing features and engineering problems under the embankments caused by

transverse thermal difference in slopes (Lai et al., 2004; Sheng et al., 2005; Dou et al., 2003; Sun, 2005). To solve the above mentioned problems is very essential, and this work will provide a scientific basis for the road construction and maintenance in the permafrost regions of the plateau. In view of the fact that the physiographical and geohydrologic conditions as well as temperature parameters of all surfaces with different roadbed strikes of Beiluhe are relatively plenty, this paper analyzes the thermal stability of the embankment with different roadbed strikes for both the gravelly and asphalt surfaces using the finite element method, taking the permafrost conditions of Beiluhe for example. Beiluhe is along the Qinghai–Tibet railway, at the South of Beiluhe Basin, belonging to diluvial alpine plain physiognomy. It is located in north latitude 34.85° and east longitude 92.94°, with elevation of 4650 m. The coverage of vegetation is less than 20%. The air mean annual temperature is −3.82 °C. Equations for thermal conduction coupled with phase transitions will be taken, so that a two-dimensional numerical model for the thermal stability with different embankment geometrical parameters is established with the assumption that the air temperature would rise by 1.1 °C/50 a on the Qinghai–Tibet plateau in the following 50 years (Li and Cheng, 1999). The finite element method will be applied for the calculation with adjustable roadbed height. The changes between the artificial permafrost table and the natural permafrost table with different embankments will be analyzed and be compared in the 20th year after roadbed construction.

2. The computational model

2.1. Governing equations and finite-element formula

Ignoring convection and mass transfer, and only considering the phase transitions and thermal conduction, the 2-D equation of thermal conduction in the soil layers can be described as follows:

$$\frac{\partial}{\partial x}\left(\lambda \frac{\partial T}{\partial x}\right) + \frac{\partial}{\partial y}\left(\lambda \frac{\partial T}{\partial y}\right) = \rho c \frac{\partial T}{\partial t} \tag{1}$$

where, ρ – soil density, T – temperature, c – volumetric thermal capacity of the soil, λ – coefficient of thermal conductivity, and t – time.

$$T_f(s(t), t) = T_u(s(T), T) = T_m \tag{2}$$

$$\lambda_f \frac{\partial T_f}{\partial n} - \lambda_u \frac{\partial T_u}{\partial n} = L\rho w_0 \frac{ds(t)}{dt} \tag{3}$$

where, f and u denote frozen and unfrozen states, respectively. L – latent thermal of water, w_0 – the initial water content, T_m – temperature on the freeze–thaw interface, n –normal direction of the freeze–thaw interface.

Latent thermal of soil can be calculated by the following equation:

$$Q = L\rho_d(w - w_u) \tag{4}$$

where, Q – the latent thermal of the soil, L – the latent thermal of water, w – the water content, and w_u – the unfrozen water content.

The unfrozen water content can be obtained by the following equations (Xu et al., 2001):

$$w_u = aT^{-b} \tag{5}$$

$$b = \frac{lnw_0 - lnw_u}{lnT - lnT_f} \tag{6}$$
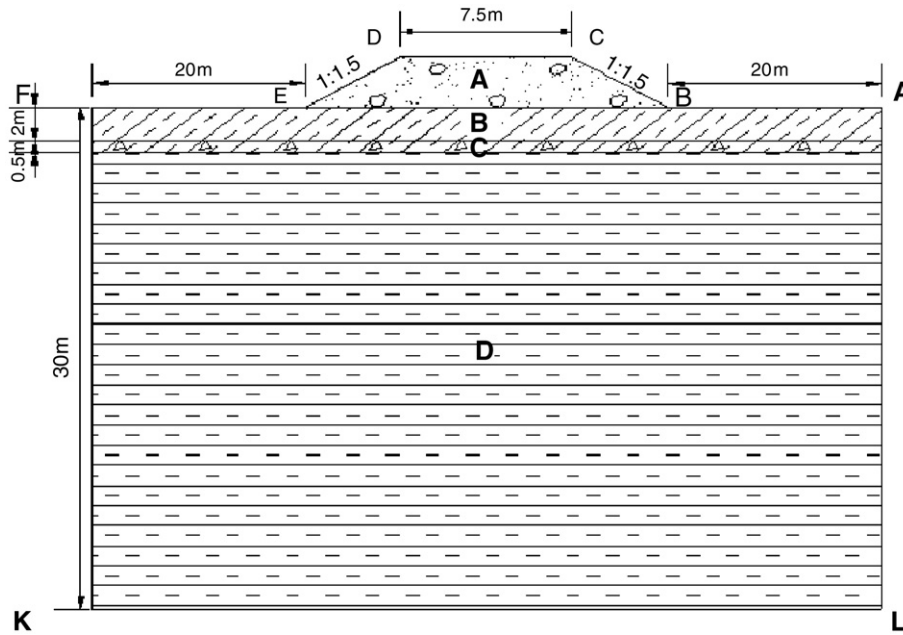
$$a = w_0 T_f^b \tag{7}$$

Fig. 1. Computational domain.

Where, T and T_f are the freezing temperatures of the soils at the initial water content w_0 and w_u, respectively.

The finite element formulas are:

$$[M]\left\{\frac{\partial T}{\partial t}\right\} + [K]\{T\} = -\{q\}$$

(8)

$$M_{ij} = \sum \int_{\Omega^e} \rho c N_i N_j d\Omega$$

(9)

$$K_{ij} = \sum \int_{\Omega^e} \lambda \left(\frac{\partial N_i}{\partial x}\frac{\partial N_j}{\partial x} + \frac{\partial N_i}{\partial y}\frac{\partial N_j}{\partial y}\right) d\Omega$$

(10)

$$q_i = \sum \int_{\Gamma_2^e} q N_i d\Gamma$$

(11)

Where, N_i and N_j are the shape functions.

2.2. Computational domain and physical parameters of soils

Although the computational domain is symmetric in terms of geometric shape with regard to the embankment central line, the shady–sunny slope problems, namely asymmetric thermal boundary conditions, have to be taken into account. The entire roadbed section has to be adopted in the calculations. Eleven embankment

heights are taken ($h = 0$, 0.5, 1.0, 1.5, 2.0, 2.5, 3.0, 3.5, 4.0, 4.5, and 5.0 m), and the physical domain for computation is extended to 20 m from the feet of the slopes and 30 m deep from the natural ground surface. The road surface width is 7.5 m, and the slope gradient is 1:1.5. The computational dimension is shown in Fig. 1, where part A is a sandy gravelly soil, part B is a silty clay, part C is a gravelly silty clay and part D is a weathered mudstone. Thermal parameters of the media are obtained from the field drilling data in Beiluhe along the Qinghai-Tibet railway, which are shown in Table 1.

2.3. Boundary conditions and initial conditions

Cheng et al. (2003) have expatiated the mean annual air temperature taken as −3.82 °C, and the mean annual temperatures and the temperature amplitudes of all the embankment surfaces with different strikes in permafrost regions in Beiluhe. Base on this, the temperature varies by the following formula:

$$T(x,y,t) = T + g(t) + A\sin\left(\frac{2\pi t}{8760} + \frac{\pi}{2}\right)$$

(12)

$$(x,y) \in \overline{AB, BC, CD, DE} \quad \text{and} \quad \overline{EF}$$

where, T – the mean annual temperatures of all the embankment surfaces, A – temperature amplitudes of all the boundaries, t – time, $\frac{\pi}{2}$ – initial phase, $g(t) = R_0 t$, R_0 – climatic warming velocity with $R_0 = 0.022$ °C/8760 h, the values of T and A are listed in Table 2.

Table 1
Thermal parameters of the materials in the computational domain.

Soil type	ρ (kg m^{-3})	λ_f (J m^{-1} °Ch^{-1})	λ_u (J m^{-1} °Ch^{-1})	C_f kJ m^{-3} °C	C_u (kJ m^{-3} °C)	Water content
Sandy gravelly soil	2100	5400	5040	1827	2226	0.08
Silty clay	1920	6480	5400	2188	2438	0.20
Gravelly silty clay	1500	7920	3600	2055	2865	0.50
Weathered mudstone	2200	9005	7200	2640	2970	0.32

Table 2
Temperature boundary conditions.

Roadbed strike	Boundary	The mean annual temperature (°C)	Amplitude (°C)
	Air	−3.82	11.5
	Natural ground surface	−1.32	12
	Gravelly surface	0.38	14.5
	Asphalt surface	2.88	15
East to west	S-slope	1.96	12.6
	N-slope	−2.26	15.5
Southwest to northeast	SE-slope	1.43	13.2
	NW-slope	−1.23	15
South to north	W-slope	0.54	13.8
	E-slope	0.1	14
Symmetric route	Slopes	0.32	13.9

Note: In the symmetric route there is no temperature difference on the two slopes.

For the lower boundary $\overline{KL}$, a temperature gradient of 0.038 °C/m is used (Zhang et al., 2005), accordingly the geothermal thermal flux is calculated as $q = 0.3079 kj/(h\ m^2)$:

$$\lambda \frac{\partial T}{\partial n} = -q \qquad (13)$$

The boundaries $\overline{FK}$ and $\overline{AL}$ are regarded as thermally insulated:

$$\lambda \frac{\partial T}{\partial n} = 0 \qquad (14)$$

The initial condition is given as:

$$T(x,y,0) = T_0 \qquad (15)$$

where, the initial temperature distribution T_0 is obtained from the following method: taking the field data under the natural ground surface of the section DK1139+670 when the air temperature is the highest as the estimated value for the computational domain temperature field, it becomes steady by Eq. (12) after an adequately long time without considering the climatic warming effect by making $g(t)=0$. The temperature distributions of this moment are considered as the initial temperature field. In the same way, the average temperature within 0.5 m under the natural ground surface is estimated as the initial temperature of roadbed filling. The position at the maximum thawed depth without considering the climatic warming effect is regarded as the original permafrost table depth. The original permafrost table in this case is −1.80 m, which is nearly consistent with the field data.

3. Computational results and analysis

In order to confirm the calculations and to demonstrate that they are representative of real conditions, comparisons of the calculated results to actual data are discussed. The calculated temperature field of the embankment on 19 Nov in the 2nd year after construction is shown in Fig. 2, whose strike is 225°. Section DK1139+970 was built in 2001, whose strike is 230°, along the Qinghai-Tibet Railway. Fig. 3 gives the temperature field of experimental cross-section DK1139+970 on 19 Nov 2002. The two embankment heights are both 4 m and the surfaces are gravelly. From the two figures, we can see that the distributions of temperature fields in experimental and calculated embankments are very similar. The tendency of 0 °C isotherms are both asymmetry, higher on the south than north.

The roadbed will meet the thermal stability on the condition that the artificial permafrost table is not lower than the natural permafrost table in the permafrost regions, based on this principle, Figs. 4 and 5 give the relations between permafrost table changes and the embankment heights in the 20th year after construction under both the gravelly and the asphalt surfaces, respectively. By analyzing all the results, it is found that there are no thaw bulbs in the embankment and the subgrade. So, the embankment heights in the calculation are not higher than the maximum critical height. Here, we discuss the minimum critical height. From Figs. 4(a) and 5(a) for the embankments with completely symmetric thermal boundary conditions, to some extent, it is seen that there are almost linear relations between the changes of the natural permafrost table and artificial permafrost table and the heights of embankment under the road in the 20th year after construction. This is in correspondence with the observed results on the Qinghai–Tibet highway and Qinghai–Kangding highway and with the numerical calculation results (Wu et al., 1988, 1998; Li et al., 1998; Huang, 1983). From the regression equations, when the running time is 20 a, the thermal-stable critical heights of embankment for asphalt and gravelly surfaces are figured out as 4.82 m and 1.22 m, respectively.

Fig. 4(b)–(d) show the relations between the changes of the permafrost table and the heights of embankment, for the east to west, the southwest to northeast and the south to north strikes respectively. It can be seen from Fig. 4 that there are hardly linear relations between the changes of natural permafrost table and artificial permafrost table and the heights of embankment for the embankments with the shady–sunny slope, under the road in the 20th year after construction. This is because for embankments with symmetric thermal boundary conditions, there is no thermal difference in the transverse direction, and the positions of the maximum thawed depths are always located in the central line of the roadbed; for embankments with the shady–sunny slope, the asymmetric thermal boundary conditions of the slopes result in that the maximum thawed depth position have
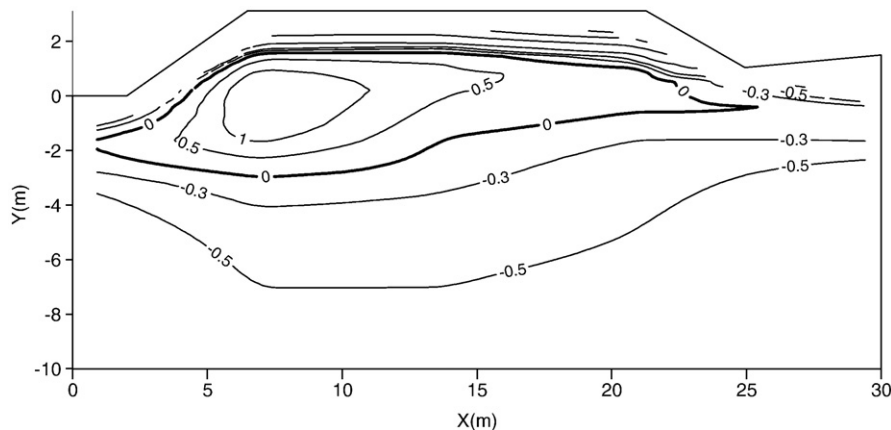

Fig. 2. Temperature field (°C) of the calculated embankment on 19 Nov in the 2nd year after construction.
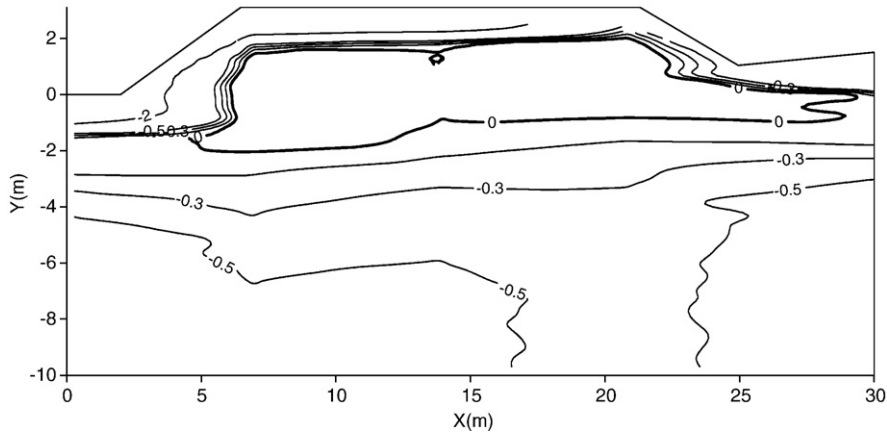
Fig. 3. Temperature field (°C)of section DK1139 + 970 on 19 Nov in the 2nd year after construction.

deviated in the transverse direction(Fig. 2). The higher is the roadbed, the greater is the transverse thermal deviation, and the weaker is the embankment thermal stability. For embankments with the south to north strike, the shady–sunny slope effect is not obvious, so the thermal-stable critical heights of embankment are not lower than 1.30 m. For embankments with the southwest to northeast strike, the thermal-stable critical height of the embankment is figured out as 1.20 m. When the embankment is higher than 2.0 m, the embankment height of the artificial permafrost table declines to a large extent with increasing of the embankment. For embankments with the west to east strike, there is no the thermal-stable critical height of embankment when the running time is 20 a. When the embankment is higher
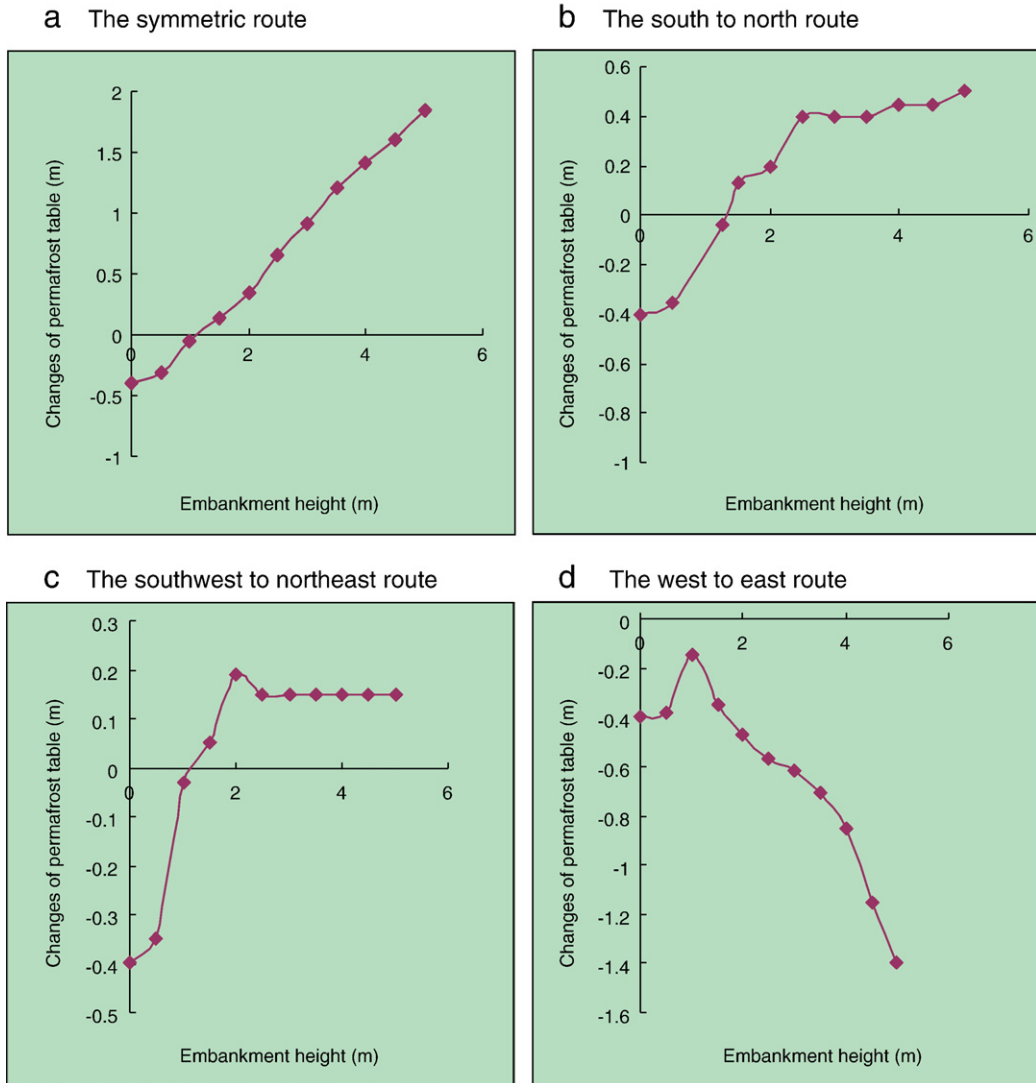

Fig. 4. Relation between the changes of the permafrost table and the embankment height under the gravelly surface (20 a).

a The symmetric route

b The south to north route

c The southwest to northeast route
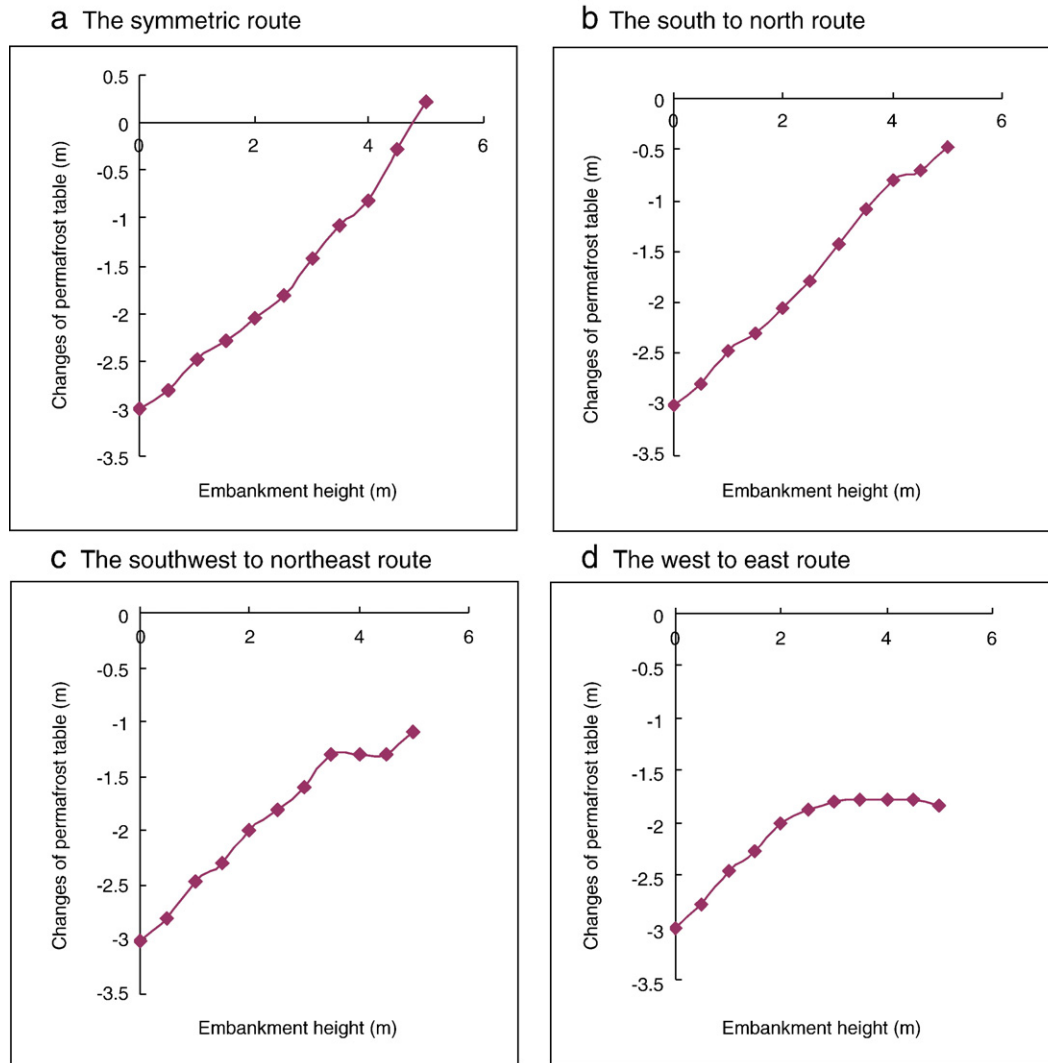
d The west to east route

Fig. 5. Relation between the changes of the permafrost table and the embankment height under the asphalt surface (20 a).

than 1.0 m, with the increase in the embankment height the artificial permafrost table is acutely declining.

It can be seen from Fig. 5(b)–(d) that, under the asphalt surface with the south to north strike, the intensive thermal absorption characteristic of the asphalt surface partially offsets the shady–sunny slope effect because the shady–sunny slope effect is not obvious, which results in that the maximum thawed depth position approx-

imates the central line of the roadbed. For embankments with the south to north strike, there are approximately linear relations between the changes of natural permafrost table and artificial permafrost table and the heights of embankment. For embankments with the southwest to northeast strike, there are almost linear relations between the changes of permafrost table and the heights of embankment when the embankment is not higher than 3.5 m. For
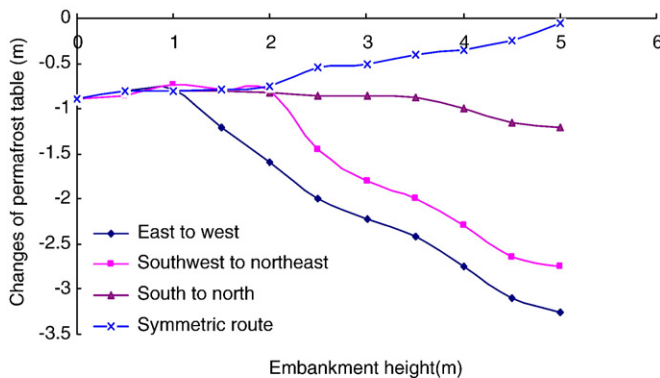
Fig. 6. Relation between the changes of the permafrost table and the embankment height under the gravelly surface (50 a).
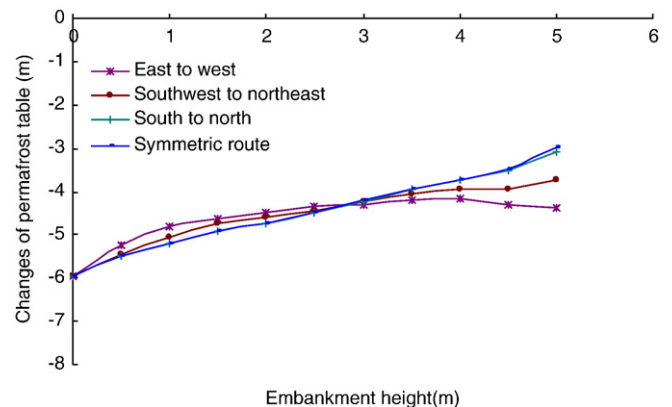
Fig. 7. Relation between the changes of the permafrost table and the embankment height under the asphalt surface (50 a).

embankments with the west to east strike, there are nearly linear relations between the changes of permafrost table and the heights of embankment when the embankment is not higher than 2.0 m. When the embankment is higher than 4.0 m, with the increase in the embankment height the artificial permafrost table is declining. The thermal stability cannot be reached under asphalt surface when the thermal boundary conditions are asymmetric.

Figs. 6 and 7 illustrate the relations between the changes of the permafrost table and the heights of embankments with different roadbed strikes in the 50th year after construction under both the gravelly and the asphalt surfaces, respectively. It can be seen that the thermal stability cannot be reached in all embankments other than the symmetric strike under the gravelly surface.

4. Conclusions

Based on the calculations and analysis, we can find several significant conclusions for the study on thermal stability of embankments with different strikes in permafrost regions.

Firstly, for the embankments with the shady–sunny slope that there are hardly linear relations between the changes of natural permafrost table and artificial permafrost table and the heights of embankment.

Secondly, there are three results when the running time is 20 a: a) with the completely symmetric thermal boundary conditions and under both the gravelly and asphalt surfaces, there are almost linear relations between the changes of permafrost table and the embankment height; b) under the gravelly surface, for embankments with sunny–shady slopes, there is no linear relation between the changes of permafrost table and the embankment height; c) under the asphalt surface, for embankments with sunny–shady slopes, if the embankment is not high enough there is a linear relation between the changes of the permafrost table and the embankment height, but the thermal stability cannot be reached.

Thirdly, when the running time is 50 a, the thermal stability of all embankments cannot be reached other than the symmetric strike under the gravelly surface.

Finally, when designing an embankment, besides considering the minimum embankment height and the maximum embankment height, the Yin-Yang Slope effect should be taken into account.

Acknowledgements

References

Cheng, G.D., 2003. The impact of local factors on permafrost distribution and its inspiring for design Qinghai-Xizang railway. Science in China (Series D) 33 (6), 602–607.

Cheng, G.D., Jiang, H., et al., 2003. Thawing index and freezing index on the embankment surface in permafrost regions. Journal of Glaciology and Geocrylogy 25 (6), 603–607.

Chou, Y.I., Sheng, Y., Li, J.P., 2007. Analysis on transverse thermal asymmetry of highway high embankment in permafrost region. Roadbed Engineering 2, 4–6.

Dou, M.J., Hu, C.S., et al., 2003. Analysis on surface troubles of the Qinghai–Tibet highway. Journal of Glaciology and Geocrylogy 24 (4), 439–444.

Hu, Zeyong, Qian, Zeyu, Cheng, Guodong, et al., 2002. Influence of solar radiation on embankment surface thermal regime of the Qinghai–Xizang railway. Journal of Glaciology and Geocrylogy 24 (2), 121–128.

Huang, X.M., 1983. Determination of the critical height of embankment for railway in permafrost regions of Tibetan Plateau. Proceedings of the Second National Conference on Permafrost (Selection). InGansu People's Publishing House, China, pp. 391–397.

Lai, Y.M., Zhang, S.J., Zhang, L.X., et al., 2004. Adjusting temperature distribution under the south and north slopes of embankment in permafrost regions by the ripped-rock revetment. Cold Region Sciences and Technology 39, 67–79.

Li, X., Cheng, G.D., 1999. A GIS-aided response model of high altitude permafrost to global change. Science in China (Series D) 29 (2), 185–192.

Li, D.Q., Wu, Z.W., Fang, J.H., et al., 1998. Heat stability analysis of embankment on the degrading permafrost district in the East of the Tibetan Plateau, China. Cold Region Sciences and Technology 28, 183–188.

Li, D.Q., Sun, Z.Z., Lai, Y.M., et al., 2005. Simulative analysis on heat stability of embankment in high temperature permafrost district of eastern Tibetan Plateau. Chinese Journal of Geotechnical Engineering 27 (12), 1376–1379.

Liu, J.K., Tian, Y.h., 2002. Numerical studies for the thermal regime of a roadbed with insulation on permafrost. Cold Region Sciences and Technology 35, 1–13.

Liu, Z.Q., Lai, Y.M., 2004. Numerical analysis of temperature field in sections of ventilation subgrade on Qinghai-Tibetan railway line[J]. Journal of Railway Engineering Society (1), 39–43.

Qinghai-Tibet Highway Research Group, 1983. Determination of the critical height of embankment for Qinghai–Tibet highway under the asphalt surface in permafrost regions. Proceedings of the Second National Conference on Permafrost (Selection). InGansu People's Publishing House, China, pp. 364–371.

Sheng, Y., Ma, Wei, Wen, Zhi, et al., 2005. Analysis of difference in thermal state between south faced slope and north faced slope of railway embankment in permafrost region. Chinese Journal of Rock Mechanics and Engineering 24 (17), 3197–3201.

Sun, Y.F., 2005. Permafrost engineering in the Qinghai–Tibet railway: research and practice. Journal of Glaciology and Geocrylogy 27 (2), 153–162.

Sun, Zengkui, Wang, Lianjun, Bai, Mingzhou, et al., 2004. Finite element analysis on temperature field of Qing–Tibet Railway embankment on permafrost. Chinese Journal of Rock Mechanics and Engineering 23 (20), 3454–3459.

Wen, Z., Sheng, Y., Ma, W., 2005. Evaluation of application of the insulation to embankment in Qinghai–Tibetan railway[J]. Journal of Glaciology and Geocrylogy 27 (5), 603–607.

Wu, Z.W., Cheng, G.D., Zhu, L.N., Liu, Y.Z., 1988. Roadbed Engineering in Permafrost Region. InPublishing House of Lanzhou University, Lanzhou, pp. 43–45.

Wu, Z.W., Zhu, L.N., Guo, X.M., et al., 1998. Critical height of the embankment in the permafrost regions along the Qinghai–Kangding highway. Journal of Glaciology and Geocrylogy 20 (1), 36–41.

Xu, X.Z., Wang, J.C., Zhang, L.X., 2001. Frozen Soil Physics. Science Press, Beijing.

Zhang, M.Y., Zhang, J.M., Lai, Y.M., 2005. Numerical analysis for critical height of railway embankment in permafrost regions of the Qinghai–Tibetan Plateau. Cold Region Sciences and Technology 41, 111–120.

Zhang, M.Y., Zhang, J.M., Liu, Z.Q., et al., 2006. Temperature characteristic nonlinear analysis for new-type embankment structures for Qinghai–Tibetan railway under climatic warming. China Civil Engineering Journal 39 (2), 93–97.